ACS OMEGA

http://pubs.acs.org/journal/acsodf

Article

Determination of Metallic Impurities in Carbon Nanotubes by Glow Discharge Mass Spectrometry

Patricia Grinberg,* Bradley A. J. Methven, Katarzyna Swider, and Zoltan Mester

Cite This: *ACS Omega* 2021, 6, 22717−22725

Read Online

ACCESS | Metrics & More | Article Recommendations

ABSTRACT: A method for the rapid assessment of metallic impurities in carbon nanotubes (CNTs) by pin-cell source geometry glow discharge mass spectrometry (GDMS) is presented. Pins were prepared by pressing CNT powder onto an indium substrate. GDMS analysis was performed using high-carbon-content nanotube and coal-certified reference materials for calibration purposes. This approach enables the calibrated measurement of 41 elemental impurities in CNTs. The method was validated by the analysis of NIST SRM 2483 single-wall CNTs (raw soot) with good agreement with the certified values. The proposed measurement approach could also be applied not only for CNTs but also for the assessment of precursor materials used in the synthesis of CNTs and for quality control during the entire manufacturing process. The ability to assess the presence of all metallic impurities in a simple, reliable, high-throughput manner will allow the industry to real-time monitor any changes in the product process, access its toxicity, and environmental impact. As sample preparation is maintained to a minimum, this allows the determination of metallic impurities at concentration levels that are usually not attainable by most techniques.

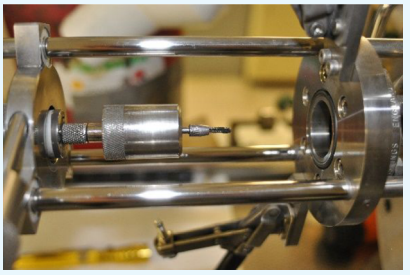

1. INTRODUCTION

Since their discovery in 1991,[1] carbon nanotubes (CNTs) have attracted a lot of interest due to their unique electronic, thermal, and mechanical properties enabled by their nanoscale structure.[2,3] CNTs are non-homogeneous materials, usually containing both amorphous and graphitic carbon along with catalytic metal impurities. These impurities could come from various sources such as the starting materials or the synthetic process or be introduced during post production manipulation. Despite extensive post-synthesis purification processes,[4] considerable variation in metal impurity still persists potentially impacting the quality and functionality of CNTs.

Characterization of the metallic impurities is of great importance not only because their presence in CNT materials can change the properties of these materials but also due to their potential impacts on environmental health and safety issues.[5−8]

Various analytical methods have been proposed for the determination of metal impurities in CNTs including spatially resolved techniques such as microscopy and bulk spectroscopic techniques.

Microscopic techniques such as transmission electron microscopy and scanning electron microscopy can often only provide a highly localized qualitative/semi-quantitative analysis of the material.[9,10]

Atomic spectroscopy methods such as inductively coupled plasma mass spectrometry (ICP−MS), optical emission spectrometry (ICP−OES), atomic absorption spectrometry,[11−18] and microwave-induced plasma optical emission spectrometry (MIP−ICP−OES)[19] are typically used for the characterization of metallic impurities in a variety of matrices. All these techniques are based on aqueous sample introduction requiring the solubilization/digestion of CNTs. However, CNTs are extremely refractory materials not amenable to conventional acid digestion procedures, thus requiring very demanding and laborious sample preparation procedures such as multistep microwave-assisted acid digestion,[15] combustion-based sample preparation,[13,14,20] or direct solid sampling[16,17] for quantitative determination. These procedures require extreme care and special clean room environments in order to avoid contamination and achieve low, reproducible blanks[15,21] while complete digestion is often not achieved.

Neutron activation analysis (NAA)[18,20] does not require sample pretreatment while offering high sensitivity; unfortunately, the accessibility of these nuclear analytical techniques is limited, making this approach unsuitable for routine or daily analysis.

X-ray fluorescence (XRF)[22−24] is another non-destructive technique (when samples do not need to be mixed with X-ray-transparent materials to form a tablet) for quantification of impurities in CNT samples but requires a large amount of the

Received: June 8, 2021
Accepted: August 6, 2021
Published: August 25, 2021

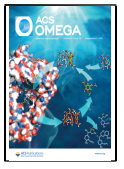

https://doi.org/10.1021/acsomega.1c03013
ACS Omega 2021, 6, 22717−22725

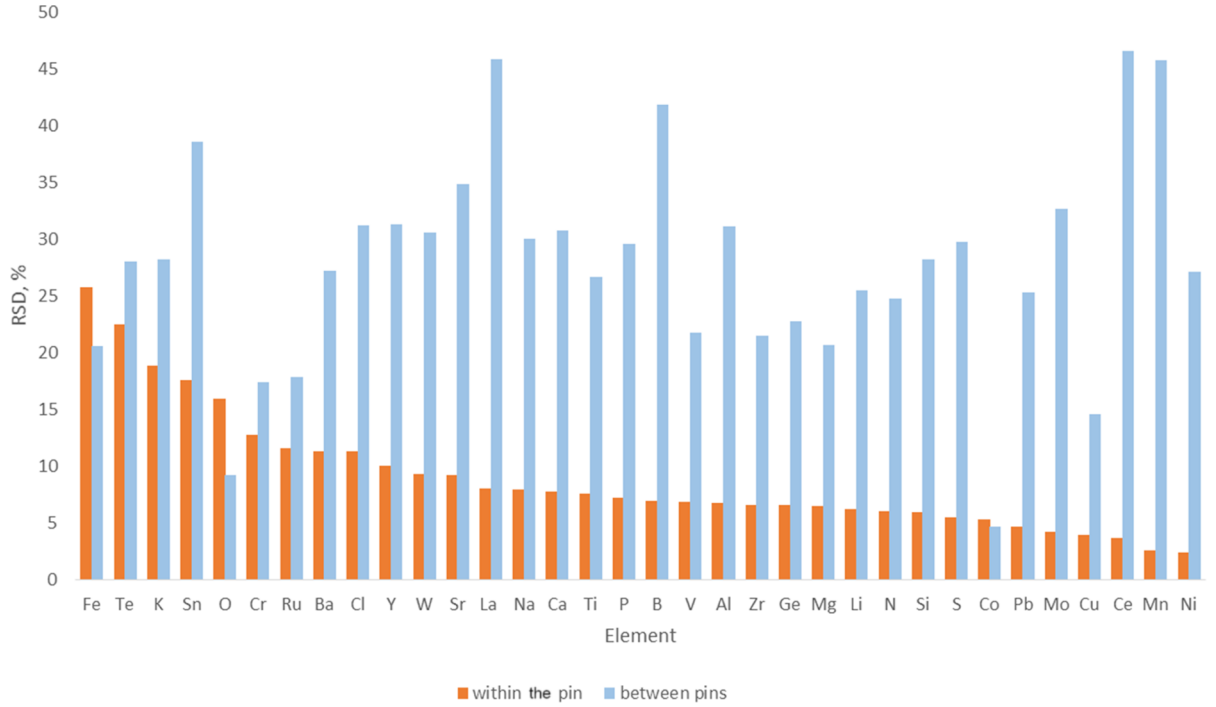

Figure 1. Reproducibility [presented as RSD (%) vs element] for the GDMS analysis of the NRC SWCNT-1 CRM.[30] Relative standard deviation (%) of the results of a single pin of In coated with SWCNT-1 CRM that was analyzed 10 times (orange box) and relative standard deviation (%) of the results of 9 different pins of In coated with SWCNT-1 CRM, with each one analyzed 5 times (blue box).

sample and has limitations to measure impurities presented at trace levels along with a limited elemental coverage.

Glow discharge mass spectrometry (GDMS) is one of the most sensitive analytical technique available for the direct determination of the elemental composition of solid materials[25−27] and is considered to be the gold standard for the analysis of trace elements in high-purity metals.[26,28] The high sensitivity of GDMS enables determination of impurities in the sample at the low/sub parts per billion level. Also, the universality of the method allows for the detection of virtually all elements in the periodic table. GDMS has several advantages such as the following:

(i) The ability to simultaneously analyze major to ultratrace levels of contaminants.
(ii) Minimum sample preparation is required as samples are analyzed directly in the solid form, therefore avoiding time-consuming chemical sample decomposition steps which can cause analyte loss and contamination, both of which are inherent to techniques relying on the wet chemical sample preparation and introduction system used in conjunction with inductively coupled plasma−mass spectrometry.
(iii) Fast analysis time.
(iv) As a direct atom ratio counting method, it has the ability to provide SI-traceable purity determination of metals.[28]

One drawback of GDMS is that it is a microsampling technique interrogating only a minute portion of the solid sample presented and, as such, inherently sensitive to sample inhomogeneity issues which could lead to a substantial increase in reported uncertainties. As there are only a limited number of reference materials/solid calibration standards available, high-precision calibration of this technique is often challenging. However, due to the nature of the ionization process, there is a fairly uniform instrumental response observed across the periodic table. This makes it possible to determine the ratio of the impurity signals to the major/matrix constituent signal with an additional minor correction factor derived from standards in a simple way.

In this study, we explore the use of GDMS for the analysis of carbon nanomaterials. The typical samples for the VG9000 model GD MS are solid, conductive, non-powdered (single-piece) pins.[28] The CNTs are powders, so approaches for sample presentation have to be developed. Knowledge of all the elemental impurities present in the CNTs will help manufacturing and determine end-user product specifications.

2. RESULTS AND DISCUSSION

Since the CNT material is in the powder form, a simple approach is required to present samples to GD analysis as powders are not inherently compatible with pin-cell GDMS. Consequently the CNT was pressed onto the surface of a high-purity indium pin. This indium pin acts as a substrate or binder for the nanotube materials.

The CNT-coated indium samples were sputtered for 20 min prior to acquisition of analytical data. During this time, the instrument was optimized for the best signal noise ratio and resolution. As the sample powder itself cannot be chemically precleaned prior to analysis (unlike a solid piece of the metal), this preburn step allows the removal of surface contamination due to sample handling and adsorbed atmospheric gases prior to analysis. After this step, the sample analysis was carried out. The entire analysis time was typically 60−90 min under discharge conditions of 800−900 V to 2.5 mA. The length of the analysis is due to the sequential nature of the high-resolution mass spectrometry data acquisition.

Using the mass balance approach in order to compute the purity of the CNT, assessment of all potential elemental

https://doi.org/10.1021/acsomega.1c03013
ACS Omega 2021, 6, 22717−22725

Table 1. List of CRMs Used for Calibration of the GDMS Instrument

analyte	# of CRMs, QC samples	CRMs and QC used: CN	CRMs and QC used: coal
Al	3	NRC SWCNT-1[30]	NIST SRM 1632d, NIST SRM 1632a
As	3		NIST SRM 1632d, NIST SRM 1632a, BCR 038
B	2	NRC SWCNT-1[30]	NIST SRM 1632d
Ba	1		NIST SRM 1632d
Ca	4	NRC SWCNT-1[30]	NIST SRM 1632d, NIST SRM 1632a, ERM-EF412
Cd	1		NIST SRM 1632a
Ce	2		NIST SRM 1632d, NIST SRM 1632a
Cl	2		NIST SRM 1632d, BCR 038
Co	4	NRC SWCNT-1[30]	NIST SRM 1632d, NIST SRM 1632a, BCR 038
Cu	4		NIST SRM 1632d, NIST SRM 1632a, BCR 038, ERM-EF412
Cr	4	NRC SWCNT-1[30]	NIST SRM 1632d, NIST SRM 1632a, BCR 038
Cs	2		NIST SRM 1632d, NIST SRM 1632a
Dy	1		NIST SRM 1632d
Eu	2		NIST SRM 1632d, NIST SRM 1632a
F	2		BCR 038, ERM-EF412
Fe	4	NRC SWCNT-1[30]	NIST SRM 1632d, NIST SRM 1632a, BCR 038
Ga	1		NIST SRM 1632a
Hf	2		NIST SRM 1632d, NIST SRM 1632a
K	3	NRC SWCNT-1[30]	NIST SRM 1632d, BCR 038
La	2	NRC SWCNT-1[30]	NIST SRM 1632d
Mg	3		NIST SRM 1632d, NIST SRM 1632a, ERM-EF412
Mn	4	NRC SWCNT-1[30]	NIST SRM 1632d, NIST SRM 1632a, BCR 038
Mo	1	NRC SWCNT-1[30]	
N	2		NIST SRM1632d, ERM-EF412
Na	5	NRC SWCNT-1[30]	NIST SRM 1632d, NIST SRM 1632a, BCR 038, ERM-EF412
Ni	5	NRC SWCNT-1[30], in-house QC-1[a]	NIST SRM 1632d, NIST SRM 1632a, BCR 038
Pb	5	NRC SWCNT-1[30]	NIST SRM 1632d, NIST SRM 1632a, BCR 038, ERM-EF412
Rb	1		NIST SRM 1632a
S	3		NIST SRM 1632d, NIST SRM 1632a, ERM-EF412
Sb	3		NIST SRM 1632d, NIST SRM 1632a, ERM-EF412
Sc	2		NIST SRM 1632d, NIST SRM 1632a
Se	1		NIST SRM 1632d
Si	1		NIST SRM 1632d
Sm	1		NIST SRM 1632d
Sr	1		NIST SRM 163da
Ti	3	NRC SWCNT-1[30]	NIST SRM 1632d, NIST SRM 1632a
Th	3		NIST SRM 1632d, NIST SRM 1632a, BCR 038
U	2		NIST SRM 1632d, NIST SRM 1632a
V	5	NRC SWCNT-1[30]	NIST SRM 1632d, NIST SRM 1632a, BCR 038, ERM-EF412
Y	1	in-house QC-1[a]	
Zn	4		NIST SRM 1632d, NIST SRM 1632a, BCR 038, ERM-EF412

[a]In-house QC-1: validated with ICP−MS analysis.

impurities is required. Purity was assessed by using the following mass balance calculation formula:[28]

$$w(M) = 1 - \sum_{i,j} [(w_M^e)_i + (0.5\ \mathrm{LOD})_j] \quad (1)$$

where $w(M)$ is the assigned purity of the matrix sample M (kg/kg) and $(w_M^e)_i$ are the individual mass fractions of each impurity element "i" present at mass fractions greater than their limit of detection (LOD). For those impurities present at or below the LOD (denoted as impurity element "j"), a rectangular distribution of values between 0 and the LOD was assumed and the value was assigned as LOD/2. This approach may lead to an overestimation of the total impurities but is generally suitable since LODs are in the ng/g range.

In was not included in impurity list as it was used as a substrate presenting to CNTs into GDMS, and it is not possible to differentiate indium originating from CNTs versus indium from the substrate.

2.1. Stability Measurement. A single pin was prepared using the procedure described in the sample preparation section from the NRC single-walled CNT certified reference material (CRM SWCNT-1).[16,29] This sample was measured 10 times in order to verify instrumental reproducibility. The time period of this analysis was over 165 min. During these measurements, the pin remained mounted in the GDMS ion source. Figure 1 shows the relative standard deviation obtained for 35 representative analytes spanning a concentration range of 280 ppb for Ce to 2.3% for O.

It was noted that for a few elements such as B, Fe, Na, and P, the concentration increases slightly over the 165 min period. Since the C matrix signal is stable over this period (2% RSD), it would indicate that the impurity concentration increases with depth. A possible explanation would be that surface-contaminated SWCNT granules that have not been sputtered clean have been exposed to the plasma. This is a notorious problem when analyzing powder samples.

It is known that analysis of powdered samples by GDMS may cause signal instabilities.[31] In our case, the signal instability is likely due to the "excess" powder being sputtered off the surface of the indium pin. It was noticed that within 1 to 2 min, the signal becomes more stable as this excess powder is removed from the pin during the initial "burn-off process". Measurements were not taken during this period. While running at a power setting of 800−900 to 2.5 mA, a signal for ^{12}C of roughly 5.5×10^{-12} amps was achieved.

CNTs are also prone to absorbing moisture.[32] During initiation of the sputtering process, any moisture presented in the sample will vaporize due to local heating, causing a temporary increase in pressure which consequently causes a voltage drop in the GD source and herein signal instability. The stability of the ^{12}C matrix signal was measured over the 165 min analysis period, which was found to be extremely stable (5.38 ± 0.12 A), representing only a 2.2% variation. Demonstrating minimal drift in the matrix signal has occurred over the course of the data acquisition process.

https://doi.org/10.1021/acsomega.1c03013
ACS Omega 2021, 6, 22717−22725

As shown in Figure 1, relative standard deviations below 10% were obtained for the majority of the analytes (26 of the 35 analytes). From the remaining nine analytes, four of them (Cr, Ru, Ba, and Cl) showed relative standard deviations between 10 and 15% and only five analytes (F, Te, K, Sn, and O) had a relative standard deviation between 15 and 26%. These results suggest that the pin integrity with regard to the overall distribution of impurities is excellent, indicating that the prepared pin is homogeneous.

The repeatability of pin preparation was also verified. Nine individual pins of CNT powder (CRM SWCNT-1) pressed onto the surface of indium were analyzed, and each of the pins was analyzed five times. The results are also presented in Figure 1.

As expected, higher pin to pin variation was observed during the analysis of nine different SWCNT-1 pins, as presented in Figure 1. RSD ranges from 5 to 45%. This increase in the RSD, when compared to only a single pin that was analyzed several times (Figure 1), is mainly due to variability introduced by the sample loading onto the pins (sample preparation) and possible variation in the CNT samples due to sample homogeneity.

It should be noted that the nine pins were prepared using three different vials of SWCNT-1 CRM. Also, certified values in the SWCNT-1 CRM were established using 25 mg of samples, and the amount used during the GDMS analysis is around 3.5 mg, which can explain the higher level of variability observed in this study.

2.2. Calibration. GDMS is considered a primary analytical method,[33] where the ratio of ion current for any impurity to the matrix is representative of the atom number ratios. The constraints of this hypothesis have been extensively evaluated and discussed elsewhere.[25,28] In brief, this theory holds firm for pin geometry GDMS instruments with a typical analyte relative uncertainty of 300% or less. If such a data quality meets the requirements of the data users (fit for purpose), then direct GDMS analysis could be considered a primary method. With this approach, there is no need for external standards, greatly simplifying the workflow of quantifying these many analytes.[28] However, to obtain more precise results (below 300% uncertainty), a relative sensitivity factor is applied to compensate for the behavioral differences observed for the various elements in the GDMS instrument.

In order to improve trueness of analysis, solid samples of known chemical compositions or CRMs could be used. In an ideal case, these solid calibrators should be similar to the analytes in terms of matrix composition. Unfortunately, only a limited number of matrix CRMs are available, and even these CRMs have only a few impurities certified. Fortunately, calibration factors for various elemental impurities vary only slightly between matrices of the same general composition, and accuracies of 15−20% could still be achieved by transferring calibration factors from matrix to matrix.[33,34]

It should be noted that calibration factors are considered constant over time as long as the ion source geometry and plasma condition are kept the same.[35]

To improve the GDMS calibration for the analysis of CNT materials, a host of CNT and coal CRMs were analyzed. There are several commercially available references materials of coal which we evaluate as proxy for CNTs, and unlike CNT CRMs, these are widely available. In this study, NIST SRM 1632d trace elements in coal (bituminous), NIST SRM 1632a trace elements in coal (bituminous), BCR038 fly ash from pulverized coal, and ERM-EF412 brown coal were used (Table 1). Although these materials were not CNTs, we demonstrate the suitability of these materials as calibrators for GDMS analysis of nanotubes. These reference materials, in conjunction with NRC SWCNT-1,[30] enable the calibrated measurement of 41 different elements in CNTs.

For most analytes, at least two CRMs were used for the instrument calibration. It was noted that for the majority of the elements, the instrument response factors obtained for the coal CRMs/QC samples were higher than the ones obtained for the CNTs, as shown in Table 2. However, the response factor ratios ranged from 0.37 to 1.21.

Table 2. Ratio of Instrument Response Factors Obtained for CNTs and Coal[a]

	instrument response factor CNT/coal
Al	1.01
B	1.21
Ba	0.70
Ca	0.55
Cl	0.81
Co	0.71
Cu	0.75
Cr	0.58
Fe	0.37
K	0.61
La	0.37
Mg	1.00
Mn	0.63
Na	0.82
Ni	0.58
Pb	0.46
Ti	0.58
V	0.65

[a]Values obtained using the CRMs/QC samples listed in Table 1.

2.3. Method Validation. The trueness of the results obtained by the proposed GDMS methodology was evaluated by analysis of a NIST SRM 2483 (single-wall CNTs). The results are summarized in Table 3 and are based on five measurements of a single pin. The results are presented as the mean ± standard deviation.

It can be seen from Table 3 that good agreement with the certified values was obtained for most of the analytes. A total of 14 values (of 17) obtained are within 20% of the certified mean value. Al and As are within 30%, and Ce and Dy are within 60%. The magnitude of these biases is consistent with the variations observed between the calibration factors observed among the CRMs used for the calibration and similar to the SWCNT-1 CRM and the recommended minimum mass of 25 mg sub-sample for NIST SRM 2483, and for the coal reference materials (i.e., NIST 1632a, NIST 1632d, BCR-038, and ERM-EF-412), the minimal mass value is 10-fold higher. As we are not capable of analyzing the material using the minimal mass amounts, homogeneity issues may be encountered.

The high sensitivity of GDMS enables the determination of impurities in the sample at the low/sub parts per billion level, thus offering orders of magnitude better sensitivity when compared to wet chemical,[11−18] XRF,[22−24] MIP−ICP−OES,[19] and other techniques.

https://doi.org/10.1021/acsomega.1c03013
ACS Omega 2021, 6, 22717−22725

Table 3. Analysis of NIST SRM 2483, Single-Wall CNTs (Raw Soot), by GDMS (n = 5)

analyte	certified value	measured value[b]	recovery (%)
Ca, %[a]	0.303	0.346 ± 0.034	88
Cl, %	0.2125 ± 0.0089	0.2635 ± 0.672	81
Co, %	0.963 ± 0.017	0.971 ± 0.036	99
Mg, %	0.1150 ± 0.0011	0.1155 ± 0.080	100
Mo, %	3.406 ± 0.029	3.24 ± 0.28	105
Na, %	0.1187 ± 0.0036	0.127 ± 0.007	93
Al, mg/kg	723 ± 19	1018 ± 45	71
As, mg/kg	12.5[a]	12.05 ± 0.6	104
B, mg/kg	74.7[a]	57.7 ± 1.9	129
Ba, mg/kg	119.0 ± 3.4	145 ± 8.3	82
Ce, mg/kg	192.7 ± 7.3	122 ± 6.7	158
Cu, mg/kg	186[a]	195 ± 1.05	95
Dy, mg/kg	8.36 ± 0.17	5.3 ± 0.64	158
Eu, mg/kg	2.27 ± 0.13	2.34 ± 0.3	97
Mn, mg/kg	4.482 ± 0.041	4.6 ± 0.2	97
Sm, mg/kg	13.09 ± 0.90	14.7 ± 0.7	89
Th, mg/kg	25.7 ± 4.4	29.8 ± 1.0	86
V, mg/kg	6.89 ± 0.14	8.11 ± 0.4	85

[a]Information value only. [b]Results presented as the mean ± standard deviation.

Table 4 represents the purity profile of biochar powder (derived from the pyrolysis of a hardwood) that was analyzed by GDMS and also by ICP−MS. Biochar is often used as a renewable precursor material for the synthesis of CNTs.[36,37]

Table 4. Analysis of a Biochar Powder Sample by GDMS and ICP−MS Using Microwave-Induced Combustion as Sample Preparation (n = 3)[a]

analyte, mg kg^{-1}	GD-MS	microwave-induced combustion with ICP−MS
Na	158 ± 4	130 ± 14
Mg	742 ± 28	521 ± 28
Al	460 ± 10	350 ± 11
Si	2300 ± 130	2442 ± 73
Ca	6000 ± 300	5066 ± 187
V	0.4 ± 0.025	3.0 ± 0.1
Cr	273 ± 6	167 ± 8
Mn	160 ± 5	160 ± 7
Fe	2100 ± 100	1514 ± 10
Ni	30 ± 0.5	30 ± 1
Co	0.6 ± 0.02	0.4 ± 0.01
Cu	11 ± 1	13 ± 0.1
Mo	3.7 ± 0.2	1.2 ± 0.1
Ba	113 ± 8	56.2 ± 0.7
Pb	2.45 ± 0.1	2.9 ± 0.1

[a]Values presented as the mean ± standard deviation. Quadrupole ICP−MS was used. GDMS data refer to data obtained during four consecutive runs of the same pin and ICP−MS to three replicates of the same sample.

In Table 4, data are reported as the mean ± standard deviation obtained during four consecutive runs of the same pin and ICP−MS to three replicates of the same sample. Microwave-induced combustion sample preparation (described in ref 15) was used in conjunction with quadrupole ICP−MS analysis. For 12 of the analytes that were analyzed, 30% or better agreement was obtained between GDMS and ICP−MS results.

The biggest discrepancies are for elements at low ppm levels such as V and Mo (although good agreement was obtained for the analysis of NIST SRM 2483). Mo is a refractory element, and this could explain the lower value obtained by the ICP−MS method, indicating incomplete digestion.

For Ba, Cr, and Fe mass fractions, it could be verified that the GDMS results were within 1.4 and 2-fold higher than those generated by microwave-induced combustion with ICP−MS. Digestion residues were visible following the microwave-induced combustion, indicating incomplete solubilization. A similar trend was previously observed[15] when comparing the mass fraction of CNT samples obtained by NAA and microwave-induced combustion with ICP−MS.

2.4. Analysis of CNT Samples. There are three main methods for the synthesis of CNTs: laser-ablation, arc-discharge, and chemical vapor deposition (CVD) methods. These methods involve gas-phase processes which provide access to the high temperature required during the synthesis of the CNTs.

In the laser-ablation method, a high-intensity laser beam is used for the sublimation of graphite and gives high-quality and high-purity nanotubes, but the drawback is the high synthesis cost. On the other hand, the arc-discharge method is considered a more cost-efficient technique for the synthesis of CNTs, and it is based on the application of a direct-current arc (formed between two graphite electrodes) immersed in an inert gas atmosphere. Both laser-ablation and arc-discharge methods were first used to synthesize CNTs and required high temperatures. These techniques have now been replaced with low-temperature CVD methods (<800 °C), where a better controlled CNT material (i.e., purity, diameter, density, orientation) can be obtained. CVD involves the application of an energy source, such as plasma or another heat source, to a carbon feedstock in the gas phase to produce CNTs on a heated (catalytic or non-catalytic) substrate. Several metals, such as Co, Y, Fe, La, Ni, and Cu, have been proposed as catalysts and for some applications such as composites, nanoelectronics, and so forth. The manufactured CNTs need to be purified post synthesis as a significant amount of the catalyst metal could be present in the final nanotube product as an impurity, potentially impacting functionality of these materials.

Table 5 presents the analysis of several CNTs, ranging from SWCNT to few-walled, double-walled, and multiwalled CNTs, and different synthesis processes. Samples were from commercial sources, and our analysis data are presented along with the information provided by the manufacturer. The majority of manufacturers determined the impurity content by thermogravimetric analysis (TGA), where the carbonaceous matrix is oxidized and the remaining residue comprises metallic impurities and their oxidation products.[38]

The overall purity claimed was reasonable for the materials. None of the manufacturers provided elemental composition data, and only one sample has information regarding Fe content (Fe < 0.1%). Knowing the elemental composition of the CNTs is paramount for some application as it can influence the properties of CNT and the behavior of devices built from these materials[39] along with associated health risk assessment.

3. CONCLUSIONS

The development of a GDMS method for the direct analysis of CNTs for elemental impurities is described, permitting a fast and reliable characterization of impurities. The analysis time of

https://doi.org/10.1021/acsomega.1c03013
ACS Omega 2021, 6, 22717−22725

Table 5. Analysis of CNT Samples[a,b]

	SWCNT (electric arc discharge)	few-walled (CoMocat)	double-walled (CVD)	multiwalled (CVD)	multiwalled (CVD)	multiwalled (CVD)
Al	45 ± 1 ppm	290 ± 6 ppm	160 ± 2 ppm	15 ± 0.4 ppm	230 ± 7 ppm	3 ± 0.1 ppm
As	<0.2 ppm	<0.1 ppm	<0.2 ppm	<0.2 ppm	<1 ppm	<0.1 ppm
B	1.3 ± 0.10 ppm	10 ± 0.2 ppm	298 ± 80 ppm	8 ± 0.3 ppm	0.1 ± 0.02%	2 ± 0.1 ppm
Ba	2.8 ± 0.7 ppm	18 ± 2 ppm	44 ± 2 ppm	100 ± 2.6 ppm	12 ± 0.3 ppm	1 ± 0.05 ppm
Ca	<0.02 ppm	60 ± 3 ppm	0.4 ± 0.01 ppm	255 ± 7.4 ppm	400 ± 12 ppm	<3 ppm
Cd	<3 ppm	34.6 ± 1 ppm	25.5 ± 1.7 ppm	<11 ppm	150 ± 50 ppm	<6 ppm
Ce	<0.2 ppm	<2 ppm	3 ppm	7 ± 0.3 ppm	21 ± 1 ppm	<0.9 ppm
Cl	260 ± 0.7 ppm	61 ± 3 ppm	358 ± 10 ppm	47 ± 1.7 ppm	390 ± 7 ppm	7 ± 0.3 ppm
Co	1.5 ± 0.3 ppm	2 ± 0.1 ppm	45 ± 0.5 ppm	1.98 ± 0.62%	400 ± 13 ppm	0.4 ± 0.01 ppm
Cu	<0.6 ppm	1.7 ± 0.1 ppm	7.9 ± 0.4 ppm	<0.3 ppm	17 ± 1 ppm	<0.2 ppm
Cr	<1 ppm	59 ± 3 ppm	15 ± 1.3 ppm	<1 ppm	<8 ppm	<2 ppm
Cs	<0.09 ppm	<0.1 ppm	<0.2 ppm	<0.3 ppm	<2.5 ppm	<0.15 ppm
Dy	<1 ppm	<0.9 ppm	<2 ppm	<2 ppm	<5 ppm	<1 ppm
Eu	<4 ppm	<4 ppm	<13 ppm	<23 ppm	<27 ppm	<9 ppm
F	<0.6 ppm	150 ± 13 ppm	<1.5 ppm	<1 ppm	830 ± 20 ppm	<0.6 ppm
Fe	1100 ± 2 ppm	0.18 ± 0.01 ppm	2.3 ± 0.4 ppm	70 ± 2 ppm	800 ± 24 ppm	100 ± 3 ppm
Ga	<0.2 ppm	<0.4 ppm	2.8 ± 0.1 ppm	<0.2 ppm	42 ± 3 ppm	1.3 ± 0.3 ppm
Hf	<0.09 ppm	<0.07 ppm	<0.2 ppm	<0.2 ppm	<0.4 ppm	<0.06 ppm
K	<4 ppm	77 ± 4 ppm	<4 ppm	<4 ppm	<6 ppm	<1 ppm
La	0.6 ± 0.03 ppm	12 ± 0.5 ppm	7.5 ± 0.6 ppm	25 ± 1 ppm	60 ± 2 ppm	45 ± 1.8 ppm
Mg	<0.7 ppm	550 ± 15 ppm	2000 ± 93 ppm	1.8 ± 0.4%	250 ± 5 ppm	<2 ppm
Mn	3 ± 0.1 ppm	12 ± 0.5 ppm	6 ± 0.3 ppm	3 ± 0.1 ppm	5 ± 0.1 ppm	<0.05 ppm
Mo	450 ± 90 ppm	0.5 ± 0.02%	2.7 ± 0.1%	9 ± 1 ppm	170 ± 15 ppm	<0.2 ppm
N	1000 ± 15 ppm	0.1 ± 0.01%	6000 ± 340 ppm	1300 ± 130 ppm	420 ± 50 ppm	330 ± 33 ppm
Na	30 ± 2 ppm	370 ± 15 ppm	220 ± 9 ppm	9 ± 0.6 ppm	670 ± 48 ppm	2 ± 0.15 ppm
Ni	23 ± 1.5%	24 ± 2 ppm	267 ± 35 ppm	25 ± 3 ppm	260 ± 15 ppm	0.95 ± 0.2 ppm
Pb	0.73 ± 0.02 ppm	<0.1 ppm	10 ± 0.5 ppm	<0.3 ppm	51 ± 1 ppm	<0.15 ppm
Rb	<0.02 ppm	<0.02 ppm	<0.02 ppm	<0.05 ppm	<0.1 ppm	<0.03 ppm
S	2.9 ± 0.1%	345 ± 11 ppm	2250 ± 90 ppm	40 ± 1.54 ppm	1300 ± 50 ppm	12 ± 0.5 ppm
Sb	<0.2 ppm	<0.2 ppm	1.3 ± 0.1 ppm	<0.4 ppm	5.6 ± 0.1 ppm	<0.2 ppm
Sc	<0.02 ppm	<0.03 ppm	<0.03 ppm	<0.04 ppm	<0.08 ppm	<0.02 ppm
Se	<2 ppm	<1 ppm	<2 ppm	<2 ppm	<9 ppm	<1 ppm
Si	455 ± 9 ppm	1000 ± 100 ppm	850 ± 48 ppm	100 ± 3 ppm	760 ± 26 ppm	25 ± 1 ppm
Sm	<1 ppm	<2 ppm	<2 ppm	<2 ppm	<6 ppm	<1 ppm
Sr	<0.1 ppm	22 ± 1 ppm	42 ± 2.6 ppm	<0.06 ppm	<0.5 ppm	<0.2 ppm
Ti	12 ± 1 ppm	20 ± 1 ppm	20 ± 1.4 ppm	10 ± 0.5 ppm	70 ± 3 ppm	4 ± 0.2 ppm
Th	<0.01 ppm	<0.02 ppm	2470 ± 150 ppm	<0.05 ppm	<0.2 ppm	<0.05 ppm
U	<0.01 ppm	<0.01 ppm	0.2 ± 0.01 ppm	<0.02 ppm	<0.05 ppm	<0.015 ppm
V	1 ± 0.1 ppm	1 ± 0.1 ppm	0.6 ± 0.05 ppm	<0.02 ppm	3.6 ± 0.2 ppm	0.17 ± 0.01 ppm
Y	2 ± 0.1%	<3 ppm	11 ± 0.3 ppm	5 ± 0.7 ppm	333 ± 50 ppm	1 ± 0.1 ppm
Zn	2 ± 0.2%	<1 ppm	100 ± 4 ppm	<2 ppm	67 ± 7 ppm	<0.7 ppm
sum of measured impurities	30.3 ± 2%	8000 ± 400 ppm	4.2 ± 0.14%	40,000 ± 7000 ppm	15,000 ± 300 ppm	540 ± 40 ppm
manufacturer impurity information	metal content 29% wt	carbon TGA 97.9%	TGA analysis residue metal oxide 6% wt	trace metal analysis ≤20,000 ppm	TGA analysis residue metal oxide ≤2% wt	impurities <5% Fe <0.1%

[a]COMOcat: combination of of cobalt and molybdenum metal particles on a silica support; CVD: chemical vapor deposition. [b]Values presented as the mean ± standard deviation.

about 1.5 h per sample is feasible, yielding a purity profile based on 60+ elements. This compares favorably to wet chemical methods or the complexity and risk associated with combustion-based sample preparation and offers orders of magnitude better sensitivity compared the wet chemical and XRF methods.

With the proposed GDMS methodology, routine analyses are possible for the metal impurities not only in the final product but also as quality control during the entire manufacturing process assessing feedstocks and intermediates.

Other carbon-based engineered (nano)materials such as carbon nanofibers,[40] graphite flakes,[41,42] graphene nanosheets,[43,44] and so forth could also benefit from this proposed methodology. Further investigation into these materials will be required.

4. EXPERIMENTAL SECTION

4.1. Instrumentation. An A VG 9000 (VG Microtrace, Windford, UK, subsequently supported by Thermo Fisher Scientific) reverse Nier−Johnson magnetic sector field double-focusing mass spectrometer was used. The instrument was

https://doi.org/10.1021/acsomega.1c03013
ACS Omega 2021, 6, 22717−22725

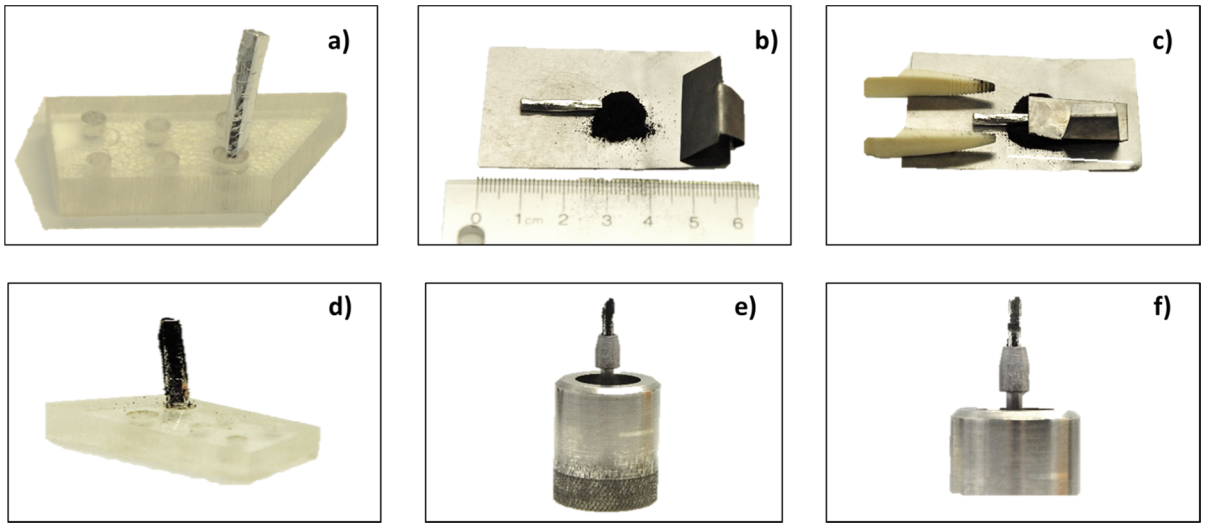

Figure 2. Sample preparation procedure: (a) 2.3 mm × 2.3 mm × 18 mm high-purity indium pin used as a substrate and binder of the nanotube material; (b) pressing the setup consisting of the In pin, a tantalum sheet (40 mm square), plastic tweezers, an L-shaped tantalum sheet, and the CNT powder sample; (c) pressing the CNT powder onto the surface of the indium; (d) CNT powder sample pressed onto the surface of the In pin; (e) CNT/In pin mounted in a clean Ta chuck before analysis; (f) CNT/In pin mounted in a clean Ta chuck after sputtering for 120 min.

fitted with a pin-source tantalum mega cell, which was cooled with liquid nitrogen in order to minimize both outgassing as the discharge heats and the formation of polyatomic interferences within the glow discharge plasma. A mass resolution of 4000 was used. A combination of Faraday and Daly detector systems, which are conveniently cross-calibrated through use of Ar isotopes from the discharge gas (^{38}Ar and ^{40}Ar), permit impurity elements to be quantitated at the ng/g mass fraction level. The Faraday ion currents lie in the range of 5×10^{-13} to 10^{-9} A, whereas the Daly is operated between 5×10^{-19} and 5×10^{-13} A. All calculations performed on raw data generated during operation are conducted using the spectrometer operating system, and thereafter, the results are exported to a laboratory information management system for report generation.

Measurements were made with a cryogenically cooled mega cell (temperature approximately −196 °C by using liquid nitrogen), and a detector dynamic range of 10^{10} can be achieved with the cross calibration of both the Faraday Cup and Daly counting systems.

The sample introduction system used for GDMS was the pin-cell geometry, which is based upon samples being analyzed in the form of pins having dimensions of roughly 18 mm in length and 2 mm in thickness. The analyte signal is obtained from a representative portion of the sample as the sputtering occurs on all four sides of the pin and its tip face.

4.2. Sample Preparation. Since the CNT material is in powder form, it was pressed onto a high-purity indium pin for GDMS analysis. This indium material acts as a substrate and binder of the nanotube material. The indium used in this exercise was 7N grade (99.99999%) purchased from Nippon Mining and Metals Company (Japan). The working pins of indium were cut down to a size of roughly 2.3 mm × 2.3 mm × 18 mm using a thin sheet of tantalum metal. The tantalum metal sheet was cleaned in a solution of high-purity sub-boiled (ultrahigh purity) nitric acid for 30 min, followed by rinsing in de-ionized water (DIW). The tantalum sheet was air-dried and cooled prior to cutting the indium pins. Each indium pin was chemically pre-cleaned prior to being used by etching the material in a solution of roughly 75% (v/v) high-purity sub-boiled nitric acid for 20 min. The pin was then rinsed with DIW, followed by vertically standing up in a small plastic holder inside a clean hood to air-dry. The indium pin is then placed onto a sheet of tantalum (a 40 mm square that has been previous cleaned using high-purity sub-boiled nitric acid), and to the top half of the indium pin, the carbon powder material is added. While holding the bottom portion of the indium pin with designated plastic tweezers, a second piece of tantalum (bent into an "L" shape) was then used as a "plunger" to press the CNT powder onto the surface of the indium. The pin was rolled over until all sides and tip were covered with the CNT powder. The sample was then mounted in a clean Ta chuck (sample holder), attached onto the end of the insertion probe, and transferred into a clean Ta discharge cell. The sample preparation procedure is presented in Figure 2.

4.3. GDMS Analysis. The GDMS sample interlock was placed under 2×10^{-2} Torr vacuum before opening the valve and exposing the sample to the high vacuum of the source chamber. The base pressure of the source and analyzer section of the instrument was 2×10^{-8} Torr. The running pressures of the source chamber and analyzer section were 1.5×10^{-4} and 1×10^{-7} Torr, respectively.

The prepared pin was placed into the cell and cooled for approximately 1 min prior to initiating the glow discharge. This was done in order to avoid the indium substrate from possibly melting when power is increased. The powder samples were sputtered using a power setting of 800−900 V and a 2.5 mA current.

Selectivity of the measurements relies on the high mass resolving power of the VG 9000 sector instrument, permitting mass-separated ion currents to be measured. Several polyatomic interferences could be presented due to the recombination of sample and matrix ions with matrix components like in the determination of ^{24}Mg (due to 2^{12}C), ^{28}Si(^{12}C^{16}O), ^{48}Ti(^{36}Ar^{12}C), ^{52}Cr(^{40}Ar^{12}C), ^{92}Mo-(2^{40}Ar^{12}C), and ^{128}Te(^{40}Ar2^{38}Ar^{12}C) among others. These possible interferences were resolved. The isotopes of specific elements were chosen for quantitation by preliminary measurements of the material using multiple isotopes for a given element and deciding which ones were interference-free

https://doi.org/10.1021/acsomega.1c03013
ACS Omega 2021, 6, 22717−22725

and also by being able to calculate the location of the interfering species via instrument software to ensure that adequate resolution/separation existed between the possible interference and the isotope of interest.

AUTHOR INFORMATION

Corresponding Author

Patricia Grinberg − *Metrology, National Research Council Canada, Ottawa, Ontario K1A 0R6, Canada;* orcid.org/0000-0002-1167-6474; Email: patricia.grinberg@nrc-cnrc.gc.ca

Authors

Bradley A. J. Methven − *Metrology, National Research Council Canada, Ottawa, Ontario K1A 0R6, Canada*

Katarzyna Swider − *Metrology, National Research Council Canada, Ottawa, Ontario K1A 0R6, Canada*

Zoltan Mester − *Metrology, National Research Council Canada, Ottawa, Ontario K1A 0R6, Canada;* orcid.org/0000-0002-2377-2615

Complete contact information is available at: https://pubs.acs.org/10.1021/acsomega.1c03013

Notes

The authors declare no competing financial interest.

REFERENCES

(1) Iijima, S. Helical microtubules of graphitic carbon. *Nature* **1991**, *354*, 56−58.

(2) Iijima, S. Carbon nanotubes: past, present, and future. *Phys. B* **2002**, *323*, 1−5.

(3) Terrones, M. Science and technology of the twenty-first century: Synthesis, Properties, and Applications of Carbon Nanotubes. *Annu. Rev. Mater. Res.* **2003**, *33*, 419−501.

(4) Rinzler, A. G.; Liu, J.; Dai, H.; Nikolaev, P.; Huffman, C. B.; Rodríguez-Macías, F. J.; Boul, P. J.; Lu, A. H.; Heymann, D.; Colbert, D. T.; Lee, R. S.; Fischer, J. E.; Rao, A. M.; Eklund, P. C.; Smalley, R. E. Large-scale purification of single-wall carbon nanotubes: process, product, and characterization. *Appl. Phys. A: Mater. Sci. Process.* **1998**, *67*, 29−37.

(5) Liu, Y.; Zhao, Y.; Sun, B.; Chen, C. Understanding the Toxicity of Carbon Nanotubes. *Acc. Chem. Res.* **2012**, *46*, 702−713.

(6) Dhawan, A.; Sharma, V. Toxicity assessment of nanomaterials: methods and challenges. *Anal. Bioanal. Chem.* **2010**, *398*, 589−605.

(7) Boverhof, D. R.; David, R. M. Nanomaterial characterization: considerations and needs for hazard assessment and safety evaluation. *Anal. Bioanal. Chem.* **2010**, *396*, 953−961.

(8) Madani, S. Y.; Mandel, A.; Seifalian, A. M. A concise review of carbon nanotube's toxicology. *Nano Rev.* **2013**, *4*, 21521.

(9) Lim, J.-H.; Bairi, V. G.; Fong, A. Quantification of impurities in carbon nanotubes: Development of ICP-MS sample preparation methods. *Mater. Chem. Phys.* **2017**, *198*, 324−330.

(10) Herrero-Latorre, C.; Álvarez-Méndez, J.; Barciela-García, J.; García-Martín, S.; Peña-Crecente, R. M. Characterization of carbon nanotubes and analytical methods for their determination in environmental and biological samples: A review. *Anal. Chim. Acta* **2015**, *853*, 77−94.

(11) Yang, K. X.; Kitto, J. P.; Swami, K.; Beach, S. E. Evaluation of sample pretreatment methods for multiwalled and single-walled carbon nanotubes for the determination of metal impurities by ICPMS, ICPOES, and instrument neutron activation analysis. *J. Anal. At. Spectrom.* **2010**, *25*, 1290−1297.

(12) Decker, J. E.; Hight Walker, A. R.; Bosnick, K.; Clifford, C. A.; Dai, L.; Fagan, J.; hooker, S.; Jakubek, Z. J.; Kingston, C.; Makar, J.; Mansfield, E.; Postek, M. T.; Simard, B.; Sturgeon, R.; Wise, S.; Vladar, A. E.; Yang, L.; Zeisler, R. Sample preparation protocols for realization of reproducible characterization of single-wall carbon nanotubes. *Metrologia* **2009**, *46*, 682−692.

(13) Pereira, J. S. F.; Antes, F. G.; Diehl, L. O.; Knorr, C. L.; Mortari, S. R.; Dressler, V. L.; Flores, E. M. M. microwave-induced combustion of carbon nanotubes for further halogen determination. *J. Anal. At. Spectrom.* **2010**, *25*, 1268−1274.

(14) Mortari, S. R.; Cocco, C. R.; Bartz, F. R.; Dresssler, V. L.; Flores, É. M. d. M. Fast digestion procedure for determination of catalyst residues in La- and Ni-based carbon nanotubes. *Anal. Chem.* **2010**, *82*, 4298−4303.

(15) Grinberg, P.; Sturgeon, R. E.; Diehl, L. d. O.; Bizzi, C. A.; Flores, E. M. M. Comparison of sample preparation techniques for determination of trace and residual catalyst metal content in SWCNT by ICP-MS. *Spectrochim. Acta, Part B* **2015**, *105*, 89−94.

(16) Resano, M.; Bolea-Fernández, E.; Mozas, E.; Flórez, M. R.; Grinberg, P.; Sturgeon, R. E. Simultaneous determination of Co, Fe, Ni and Pb in carbon nanotubes by means of solid sampling high resolution continuum source graphite furnace atomic absorption spectrometry. *J. Anal. At. Spectrom.* **2013**, *28*, 657−665.

(17) Mello, P. A.; Rodrigues, L. F.; Nunes, M. A. G.; Mattos, J. C. P.; Müller, E. I.; Dressler, V. L.; Flores, E. M. M. Determination of metal impurities in carbon nanotubes by direct solid sampling electrothermal atomic absorption spectrometry. *J. Braz. Chem. Soc.* **2011**, *22*, 1040−1049.

(18) Ge, C.; Lao, F.; Li, W.; Li, Y.; Chen, C.; Qiu, Y.; Mao, X.; Li, B.; Chai, Z.; Zhao, Y. Quantitative Analysis of metal impurities in carbon nanotubes: efficacy of different pretreatment protocols for ICPMS spectroscopy. *Anal. Chem.* **2008**, *80*, 9426−9434.

(19) Li, M.; Deng, Y.; Jiang, X.; Hou, X. UV photochemical vapor generation-nitrogen microwave induced plasma optical emission spectrometric determination of nickel. *J. Anal. At. Spectrom.* **2018**, *33*, 1086−1091.

(20) Zeisler, R.; Paul, R. L.; Oflaz Spatz, R.; Yu, L. L.; Mann, J. L.; Kelly, W. R.; Lang, B. E.; Leigh, S. D.; Fagan, J. Elemental analysis of a single-wall carbon nanotube candidate reference material. *Anal. Bioanal. Chem.* **2011**, *399*, 509−517.

(21) Kučera, J.; Bennet, J. W.; Oflaz, R.; Paul, R. L.; Fernandes, E. A. D. N.; Kubesova, M.; Bacchi, M. A.; Stopic, A. J.; Sturgeon, R. E.; Grinberg, P. Elemental Characterization of Single-Wall Carbon Nanotube Certified Reference Material by Neutron and Prompt γ Activation Analysis. *Anal. Chem.* **2015**, *87*, 3699−3705.

(22) Cavness, B.; Heimbecker, J.; Velasquez, J.; Williams, S. X-ray fluorescence as a method of monitoring metal catalyst content during the purification of carbon nanotubes. *Radiat. Phys. Chem.* **2012**, *81*, 131−134.

(23) Das, R.; Hamid, S. B. A.; Ali, M. E.; Ramakrishna, S.; Yongzhi, W. Carbon Nanotubes Characterization by X-ray Powder Diffraction − A Review. *Curr. Nanosci.* **2015**, *11*, 23.

(24) Zhdanov, A. A.; Kazakova, M. A. Use of Carbon Materials of Different Nature in Determining Metal Concentrations in Carbon Nanotubes by X-Ray Fluorescence Spectrometry nickel. *J. Anal. At. Spectrom.* **2020**, *75*, 312−319.

(25) Mykytiuk, A. P.; Semeniuk, P.; Berman, S. Analysis of high purity metals and semiconductor materials by glow discharge mass spectrometry. *Spectrochim. Acta Rev.* **1990**, *13*, 1−10.

(26) Hoffmann, V.; Kasik, M.; Robinson, P. K.; Venzago, C. Glow discharge mass spectrometry. *Anal. Bioanal. Chem.* **2005**, *381*, 173−188.

(27) Winchester, M. R.; Payling, R. Radio-frequency glow discharge spectrometry: *Spectrochim. Acta, Part B* **2004**, *59*, 607−666.

(28) Sturgeon, R. E.; Methven, B.; Willie, S. N.; Grinberg, P. Assignment of purity to primary metal calibrants using pin-cell VG 9000 glow discharge mass spectrometry: a primary method with direct traceability to the SI international system of units? *Metrologia* **2014**, *51*, 410−422.

(29) Grinberg, P.; Ralph, S.; Indu, P. G.; Juris, M.; Scott, W. *SWCNT-1: Single-Wall Carbon Nanotube Certified Reference Material*; National Research Council Canada: Ottawa, 2013.

(30) Grinberg, P.; Sturgeon, R.; Pihillagawa, I. G.; Meija, J.; Willie, S. SWCNT-1: Single-Wall Carbon Nanotube Certified Reference Material. In *Canadian Reference Materials and Methods*; National Research Council of Canada: Ottawa, Canada, 2013.
(31) Gusarova, T.; Methven, B.; Kipphardt, H.; Sturgeon, R.; Matschat, R.; Panne, U. Calibration of double focusing glow discharge mass spectrometry instruments with pin-shaped synthetic standards. *Spectrochim. Acta, Part B* **2011**, *66*, 847−854.
(32) Sturgeon, R. E.; Lam, J. W.; Windust, A.; Grinberg, P.; Zeisler, R.; Oflaz, R.; Lang, B. E.; Fagan, J. A.; Simard, B.; Kingston, C. T. Determination of moisture content of single-wall carbon nanotubes. *Anal. Bioanal. Chem.* **2012**, *402*, 429−438.
(33) King, F. L.; Teng, J.; Steiner, R. E. Glow Discharge Mass Spectrometry: trace element determinations in solid samples. *J. Anal. At. Spectrom.* **1995**, *30*, 1061−1075.
(34) Vieth, W.; Huneke, J. C. Relative sensitivity factors in glow discharge mass spectrometry. *Spectrochim. Acta, Part B* **1991**, *46*, 137−153.
(35) Venzago, C.; Weigert, M. Application of the glow discharge mass spectrometry (GDMS) for the multi-element trace and ultratrace analysis of sputtering targets. *Fresenius. J. Anal. Chem.* **1994**, *350*, 303.
(36) Hidalgo, P.; Navia, R.; Hunter, R.; Coronado, G.; Gonzalez, M. Synthesis of carbon nanotubes using biochar as precursor material under microwave irradiation. *J. Environ. Manage.* **2019**, *244*, 83−91.
(37) Zhang, J.; Tahmasebi, A.; Omoriyekomwan, J. E.; Yu, J. Production of carbon nanotubes on bio-char at low temperature via microwave-assisted CVD using Ni catalyst. *Diamond Relat. Mater.* **2019**, *91*, 98−106.
(38) Mansfield, E.; Kar, A.; Hooker, S. A. Applications of TGA in quality control of SWCNTs. *Anal. Bioanal. Chem.* **2010**, *396*, 1071−1077.
(39) Ge, C.; Li, Y.; Yin, J.-J.; Liu, Y.; Wang, L.; Zhao, Y.; Chen, C. The contributions of metal impurities and tube structure to the toxicity of carbon nanotube materials. *NPG Asia Mater.* **2012**, *4*, No. e32.
(40) Lee, K. H.; Lee, S. H.; Ruoff, R. S. Synthesis of Diamond-Like Carbon Nanofiber Films. *ACS Nano* **2020**, *14*, 13663−13672.
(41) Lai, J.; Guo, H.; Wang, Z.; Li, X.; Zhang, X.; Wu, F.; Yue, P. Preparation and characterization of flake graphite/silicon/carbon spherical composite as anode materials for lithium-ion batteries. *J. Alloys Compd.* **2012**, *530*, 30−35.
(42) Wissler, M. Graphite and carbon powders for electrochemical applications. *J. Power Sources* **2006**, *156*, 142−150.
(43) Guo, H.-L.; Wang, X.-F.; Qian, Q.-Y.; Wang, F.-B.; Xia, X.-H. A Green Approach to the Synthesis of Graphene Nanosheets. *ACS Nano* **2009**, *3*, 2653−2659.
(44) Choucair, M.; Thordarson, P.; Stride, J. A. Gram-scale production of graphene based on solvothermal synthesis and sonication. *Nat. Nanotechnol.* **2008**, *4*, 30−33.

https://doi.org/10.1021/acsomega.1c03013
ACS Omega 2021, 6, 22717−22725